# On the Robustness of Space-Time Coding Techniques Based on a General Space-Time Covariance Model

Larry T. Younkins, *Member, IEEE*, Weifeng Su, *Member, IEEE*, and K. J. Ray Liu, *Fellow, IEEE*

***Abstract*—The robustness of space-time coding techniques for wireless channels that exhibit both temporal and spatial correlation is investigated. A general space-time covariance model is developed and employed to evaluate the exact pairwise error probability for space-time block codes. The expressions developed for the pairwise error probability are used in conjunction with the union bound to determine an upper bound for the probability of a block error. The block error probability is evaluated for several space-time codes and for wireless channels that exhibit varying degrees of spatial and temporal correlation. Numerical results are presented for a two-dimensional Gaussian scatterer model which has been shown to be consistent with recent field measurements of wireless channels. The results demonstrate that the best-case wireless channel is uncorrelated in both space and time. Correlation between transmission paths, due to insufficient spacing of the transmit antennas or scatterers located in close proximity to the mobile, can result in a significant performance degradation. The conditions that result in uncorrelated transmission paths are quantified in terms of the effective scattering radius and the spacing of the transmit and receive antennas.**

***Index Terms*—Receiver diversity, space-time coding, transmitter diversity, wireless channels, wireless communications.**

## I. Introduction

WIRELESS systems employing multiple transmit and receive antennas have the potential for tremendous gains in channel capacity through exploitation of independent transmission paths due to scattering. Transmit diversity, achieved through the use of space-time coding techniques at the base station, is a recent innovation motivated by the need for higher throughput in the wireless channel. A simple two-branch transmit diversity scheme was proposed by Alamouti [1]. It was demonstrated that this scheme provides the same diversity order as a wireless system employing a single transmit antenna and two receive antennas and utilizing maximal-ratio combining (i.e., classical receive diversity). The bit error rate performance of the proposed scheme was evaluated assuming that the path from each transmit antenna to each receive antenna experiences mutually uncorrelated Rayleigh amplitude fading. Abundant space-time codes to achieve transmit diversity have been proposed, for example, see [2]–[5] and the references therein. In these works, a Rayleigh channel model was used to evaluate the performance of the proposed codes and the transmit antennas were assumed to be sufficiently spaced such that the transmission paths are independent.

The majority of the research to date on space-time coding techniques has employed the assumption of uncorrelated transmission paths without regard for the conditions under which this assumption is justified. The degree of correlation between channel transmission paths from a transmit antenna to a receive antenna depends significantly on the scattering environment and on the antenna separation at the transmitter and receiver. For example, if the majority of the channel scatterers are located in close proximity to the mobile, then the transmission paths will be highly correlated unless the transmit antennas are sufficiently separated in space.

In recently published work, Wang *et al.* [6] derive the exact pairwise error probability for space-time coding over quasi-static or fast-fading Rayleigh channels in the presence of spatial fading correlation. For analytical tractability, the authors assume the channel matrix can be decomposed as a product of the square roots of the transmit and receive correlation matrices, respectively. The effects of spatial correlation on space-time coding performance are investigated for several scenarios, but it is unclear how the parameters chosen relate to physical scattering parameters such as effective scattering radius, etc.

Early research that characterized the spatial and temporal characteristics of the mobile radio channel was performed by Jakes [7] and Clarke [8]. In these works, a geometric scattering model was employed that places scatterers uniformly on a circular ring a fixed distance from the mobile. More recently, Chen *et al.* [9] extended this circular ring scatterer model to include multiple antennas at the base station, a single antenna at the mobile, and Doppler effects due to motion of the mobile. An example illustrating the effects of spatial and temporal correlation on antenna spacing and interleaving depth was given for a simple space-time repetition code. Shiu *et al.* [10] investigated the effects of fading correlation on the capacity of multiple-antenna wireless systems by employing the Jakes model to multiple antennas at the base station as well as the mobile. However, Doppler effects due to mobile motion were not considered. Abdi [11] developed a space-time correlation model for multiple antenna wireless systems by employing the circular ring scattering geometry but allowing a non uniform distribution of scatterers. Specifically, the von Mises density was used to describe the angle of arrival of the multipath with respect to the mobile. Doppler effects are included in this model.

Manuscript received February 12, 2004; revised July 27, 2004, January 17, 2005. This work was supported in part by the U.S. Army Research Laboratory under Cooperative Agreement DAAD 190120011. The review of this paper was coordinated by Prof. M. Juntti.

L. T. Younkins is with the Applied Physics Laboratory, Johns Hopkins University, Laurel, MD 20723 USA (e-mail: larry.younkins@jhuapl.edu).

W. Su is with the Department of Electrical Engineering, State University of New York, Buffalo, NY 14260 USA (e-mail: weifeng@eng.buffalo.edu).

K. J. R. Liu is with the Departnent of Electrical and Computer Engineering, University of Maryland, College Park, MD 20742 USA (e-mail: kjrliu@eng.umd.edu).

Digital Object Identifier 10.1109/TVT.2005.861181

0018-9545/$20.00 © 2006 IEEE

Independently, Safar [12] derived a special case of this model in which the angle of arrival was uniformly distributed.

What is currently needed is an evaluation of space-time coding performance for wireless channels that exhibit both spatial and temporal correlation. Additionally, the channel model should be parameterized to permit investigation over a wide range of wireless channels. In the work presented here, we develop a general space-time covariance model based upon scatterer geometry, transmit and receive antenna geometry, and a linear motion model for the mobile. The model is applicable to arbitrary scatterer geometry and includes Doppler effects due to mobile motion. The covariance model is evaluated for a two-dimensional (2-D) Gaussian scattering model and is used to quantify the performance of space-time coding techniques for wireless channels that exhibit both temporal and spatial correlation. The conditions under which the transmission paths can be considered to be uncorrelated are quantified in terms of the required antenna spacing and scattering radius. Additionally, the block error probability is evaluated for several space-time codes in terms of physical parameters such as transmit and receive antenna spacing, scattering radius, and normalized Doppler frequency.

The paper is organized as follows. The channel model is presented in Section II followed by the derivation of the exact pairwise error probability for space-time codes. Details of the space-time covariance model are presented in Section III. Numerical results that illustrate the block error probability for several space-time codes with varying scattering conditions are presented in Section IV followed by the conclusions.

## II. Channel Model and Pairwise Error Probability

Consider a wireless system employing $M$ transmit antennas and $N$ receive antennas. The signal received at the $q$th antenna at time $t$ is

$$y_q(t) = \sqrt{\frac{\rho}{M}} \sum_{p=1}^{M} h_{p,q}(t) c_p(t) + z_q(t) \tag{1}$$

where $h_{p,q}(t)$ is the complex path gain between the $p$th transmit antenna and the $q$th receive antenna at time $t$ and is modeled as complex Gaussian with zero mean and unit variance. $c_p(t)$ denotes the space-time code symbol transmitted by the $p$th antenna at time slot $t$, and $z_q(t)$ is independent complex Gaussian noise with zero mean and unit variance. In (1), $\rho$ denotes the signal-to-noise ratio (SNR) per receive antenna. Each space-time signal is described by a $T \times M$ matrix $\mathbf{C}$ with the columns corresponding to the space dimension and the rows corresponding to the time dimension

$$\mathbf{C} = \begin{pmatrix} c_1(1) & c_2(1) & \cdots & c_M(1) \\ c_1(2) & c_2(2) & \cdots & c_M(2) \\ \vdots & \vdots & \ddots & \vdots \\ c_1(T) & c_2(T) & \cdots & c_M(T) \end{pmatrix}. \tag{2}$$

The space-time code symbol $c_p(t)$ is chosen as the entry in the code matrix corresponding to the $p$th column and $t$th row. The space-time signal is transmitted over $T$ time slots and employs $M$ transmit antennas.

Equation (1) can be rewritten in vector form as [14]

$$\mathbf{Y} = \sqrt{\frac{\rho}{M}} \mathbf{D}\mathbf{H} + \mathbf{Z} \tag{3}$$

where the $NT \times MNT$ matrix $\mathbf{D}$ is constructed from the space-time signal matrix $\mathbf{C}$ as follows:

$$\mathbf{D} = \begin{pmatrix} D_1 & D_2 & \cdots & D_M & \cdots & 0 & 0 & \cdots & 0 \\ 0 & 0 & \cdots & 0 & \cdots & 0 & 0 & \cdots & 0 \\ & & \vdots & & \ddots & & & \vdots & \\ 0 & 0 & \cdots & 0 & \cdots & D_1 & D_2 & \cdots & D_M \end{pmatrix} \tag{4}$$

with

$$D_i = \mathrm{diag}(c_i(1), c_i(2), \ldots, c_i(T)), \quad i = 1, 2, \ldots, M. \tag{5}$$

The $MNT \times 1$ channel vector $\mathbf{H}$ is defined by

$$\mathbf{H} = (\mathbf{h}'_{1,1}, \ldots, \mathbf{h}'_{M,1}, \cdots, \mathbf{h}'_{1,N}, \ldots, \mathbf{h}'_{M,N})' \tag{6}$$

with

$$\mathbf{h}_{i,j} = (h_{i,j}(1), h_{i,j}(2), \ldots, h_{i,j}(T))' \tag{7}$$

and $'$ denoting the matrix transpose operation. The $NT \times 1$ received signal vector $\mathbf{Y}$ is defined by

$$\mathbf{Y} = (y_1(1), \ldots, y_1(T), \ldots, y_N(1), \ldots, y_N(T))' \tag{8}$$

and the $NT \times 1$ noise vector $\mathbf{Z}$ is given by

$$\mathbf{Z} = (z_1(1), \ldots, z_1(T), \ldots, z_N(1), \ldots, z_N(T))'. \tag{9}$$

Suppose $\mathbf{D}_\alpha$ and $\mathbf{D}_\beta$ correspond to two distinct space-time signals $\mathbf{C}_\alpha$ and $\mathbf{C}_\beta$, respectively. Assuming the channel matrix $\mathbf{H}$ is known, the hypothesis test for choosing between $\mathbf{C}_\alpha$ and $\mathbf{C}_\beta$ is

$$\left(\mathbf{Y} - \sqrt{\frac{\rho}{M}}\mathbf{D}_\alpha\mathbf{H} + \mathbf{Z}\right)^\dagger \left(\mathbf{Y} - \sqrt{\frac{\rho}{M}}\mathbf{D}_\alpha\mathbf{H} + \mathbf{Z}\right) \underset{\mathbf{C}_\alpha}{\overset{\mathbf{C}_\beta}{\gtrless}} \left(\mathbf{Y} - \sqrt{\frac{\rho}{M}}\mathbf{D}_\beta\mathbf{H} + \mathbf{Z}\right)^\dagger \left(\mathbf{Y} - \sqrt{\frac{\rho}{M}}\mathbf{D}_\beta\mathbf{H} + \mathbf{Z}\right) \tag{10}$$

where the symbol $\dagger$ denotes the matrix conjugate transpose operation. This test corresponds to choosing between two (complex) Gaussian vectors with equal covariance matrices and unequal mean vectors. The pairwise error probability given the channel vector $\mathbf{H}$ is [15]

$$\Pr(\mathbf{C}_\alpha \to \mathbf{C}_\beta | \mathbf{H}) = \mathrm{Q}\left(\sqrt{\frac{\rho}{2M} \|(\mathbf{D}_\alpha - \mathbf{D}_\beta)\mathbf{H}\|^2}\right) \tag{11}$$

where $\|\mathbf{x}\|$ denotes the norm of the vector $\mathbf{x}$; i.e., $\|\mathbf{x}\|^2 = \mathbf{x}^\dagger\mathbf{x}$ and $Q(x)$ denotes the Gaussian Q function. An alternative form of the Gaussian Q function due to Craig [16] is employed in the sequel. It is defined as

$$\begin{aligned} \mathrm{Q}(x) &= \frac{1}{\sqrt{2\pi}} \int_x^\infty \exp(-t^2/2)\, dt \\ &= \frac{1}{\pi} \int_0^{\pi/2} \exp\left(-\frac{x^2}{2\sin^2\theta}\right) d\theta. \end{aligned} \tag{12}$$

Considering now the expectation over the channel vector $\mathbf{H}$, we have

$$\begin{aligned}\Pr(\mathbf{C}_\alpha \to \mathbf{C}_\beta) &= E\left\{Q\left(\sqrt{\frac{\rho}{2M}\|(\mathbf{D}_\alpha - \mathbf{D}_\beta)\mathbf{H}\|^2}\right)\right\} \\ &= \frac{1}{\pi}\int_0^{\pi/2} E\left\{\exp\left(-\frac{\rho}{M}\frac{\|(\mathbf{D}_\alpha - \mathbf{D}_\beta)\mathbf{H}\|^2}{4\sin^2\theta}\right)\right\} d\theta.\end{aligned} \tag{13}$$

Assuming that the channel vector $\mathbf{H}$ is complex Gaussian with zero mean vector and covariance matrix $\mathbf{R}$, a result due to Turin [17], [18] regarding the characteristic function of a quadratic form of a complex Gaussian vector may be used to evaluate the expectation appearing in (13)

$$\begin{aligned}&E\left\{\exp\left(-\frac{\rho}{M}\frac{\|(\mathbf{D}_\alpha - \mathbf{D}_\beta)\mathbf{H}\|^2}{4\sin^2\theta}\right)\right\} \\ &= \frac{1}{\det\left(\mathbf{I} + \frac{\rho}{M}\frac{(\mathbf{D}_\alpha - \mathbf{D}_\beta)\mathbf{R}(\mathbf{D}_\alpha - \mathbf{D}_\beta)^\dagger}{4\sin^2\theta}\right)} \\ &= \prod_{i=1}^{K}\left(1 + \frac{\rho}{M}\frac{\lambda_i}{4\sin^2\theta}\right)^{-1}\end{aligned} \tag{14}$$

with $K$ corresponding to the rank of the matrix

$$(\mathbf{D}_\alpha - \mathbf{D}_\beta)\mathbf{R}(\mathbf{D}_\alpha - \mathbf{D}_\beta)^\dagger \tag{15}$$

and $\{\lambda_i\}_{i=1}^K$ its eigenvalues. The final expression for the pairwise error probability between $\mathbf{C}_\alpha$ and $\mathbf{C}_\beta$ is now given by

$$\Pr(\mathbf{C}_\alpha \to \mathbf{C}_\beta) = \frac{1}{\pi}\int_0^{\frac{\pi}{2}}\prod_{i=1}^{K}\left(1 + \frac{\rho}{M}\frac{\lambda_i}{4\sin^2\theta}\right)^{-1} d\theta. \tag{16}$$

Given space-time codes $\mathbf{C}_\alpha$ and $\mathbf{C}_\beta$ and the channel (space-time) covariance matrix $\mathbf{R} = E\{\mathbf{H}\mathbf{H}^\dagger\}$, the pairwise error probability can be calculated from (16).

An upper bound on the probability of incorrectly decoding a space-time block code may be obtained by employing the union bound. Specifically, let $\mathrm{P}_{\mathrm{block}}$ denote the probability that the space-time block code is erroneously decoded. Then,

$$\mathrm{P}_{\mathrm{block}} \le \sum_\alpha \Pr(\mathbf{C}_\alpha)\sum_{\alpha\ne\beta}\Pr(\mathbf{C}_\alpha \to \mathbf{C}_\beta). \tag{17}$$

In the sequel, the expression for the upper bound on the block error probability (17) is evaluated to assess space-time code performance. Define the diversity order $\delta$ as

$$\delta = \lim_{\rho\to\infty}\frac{\log \mathrm{P}_{\mathrm{block}}}{\log\rho}. \tag{18}$$

The parameter $\delta$ describes the asymptotic slope of the block error probability versus SNR. For example, a diversity order of two implies a reduction of $10^{-2}$ in the block error probability for each 10 dB increase in SNR. In the sequel, the achieved diversity order is also used to assess space-time code performance.

## III. Space-Time Covariance Model

In this section, we present a space-time covariance model that is applicable to arbitrary scatterer geometry, multiple antennas at the base station and the mobile, and includes Doppler effects due to mobile motion. The resulting model is then evaluated for the special case of the circular ring scattering geometry.

The complex path gain between the $p$th antenna at the base and the $q$th antenna at the mobile is denoted by $h_{p,q}(t)$. It consists of contributions from $K$ discrete scatterers with the $m$th scatterer characterized by its amplitude $A_m$, phase $\psi_m$, and spatial location $\vec{x}_m$. All scatterers are assumed to be coplanar with the mobile and base station. The spatial locations of the array phase centers for the mobile and base are $\vec{x}_{\mathrm{mobile}}$ and $\vec{x}_{\mathrm{base}}$, respectively. The spatial location of the $p$th antenna at the base is denoted by $\vec{x}^p_{\mathrm{base}}$ and the spatial location of the $q$th antenna at the mobile is denoted by $\vec{x}^q_{\mathrm{mobile}}$. Fig. 1 illustrates the geometry for the scattering model. Assuming a plane wave with frequency $f_c$ is transmitted by the base, the expression for the complex path gain $h_{p,q}(t)$ is

$$\begin{aligned}h_{p,q}(t) = &\sum_{m=0}^{K-1} A_m \exp(j\psi_m)\exp[-j2\pi f_c\tau_m(t)] \\ &\times \exp\left[+j\vec{k}^m_{\mathrm{base}}\cdot\vec{x}^p_{\mathrm{base}} + j\vec{k}^m_{\mathrm{mobile}}\cdot\vec{x}^q_{\mathrm{mobile}}\right].\end{aligned} \tag{19}$$

In the previous expression, $\tau_m(t)$ denotes the path delay associated with the $m$th scatterer and

$$\vec{k}^m_{\mathrm{mobile}} = \frac{2\pi}{\lambda}(\cos\theta_m, \sin\theta_m, 0) \tag{20}$$

$$\vec{k}^m_{\mathrm{base}} = \frac{2\pi}{\lambda}(\cos\phi_m, \sin\phi_m, 0) \tag{21}$$

with $\lambda$ denoting the transmitted wavelength. The angle $\theta_m$ corresponds to the angle of arrival at the mobile associated with the signal reradiated from the $m$th scatterer. The angle $\phi_m$ corresponds to the angle of departure from the base associated with the $m$th scatterer. The expression for the correlation between the transmission paths associated with the signal received at the $q$th element of the mobile array and transmitted from the $p$th element of the base array and the signal received by the $s$th element of the mobile array and transmitted from the $r$th element of the base array at time lag $\Delta t$ is

$$\begin{aligned}&E\{h_{p,q}(t)h^*_{r,s}(t+\Delta t)\} \\ &= E\left\{\sum_{m=0}^{K-1}\sum_{n=0}^{K-1} A_m A_n \exp(j\psi_m - j\psi_n)\right. \\ &\quad\times\exp[j2\pi f_c(-\tau_m(t) + \tau_n(t+\Delta t))] \\ &\quad\times\exp\left[+j\vec{k}^m_{\mathrm{base}}\cdot\vec{x}^p_{\mathrm{base}} + j\vec{k}^m_{\mathrm{mobile}}\cdot\vec{x}^q_{\mathrm{mobile}}\right] \\ &\quad\left.\times\exp\left[-j\vec{k}^n_{\mathrm{base}}\cdot\vec{x}^r_{\mathrm{base}} - j\vec{k}^n_{\mathrm{mobile}}\cdot\vec{x}^s_{\mathrm{mobile}}\right]\right\}.\end{aligned} \tag{22}$$

Assuming the phases associated with the $m$th and $n$th scatterers $\psi_m$ and $\psi_n$, are independent and uniformly distributed on

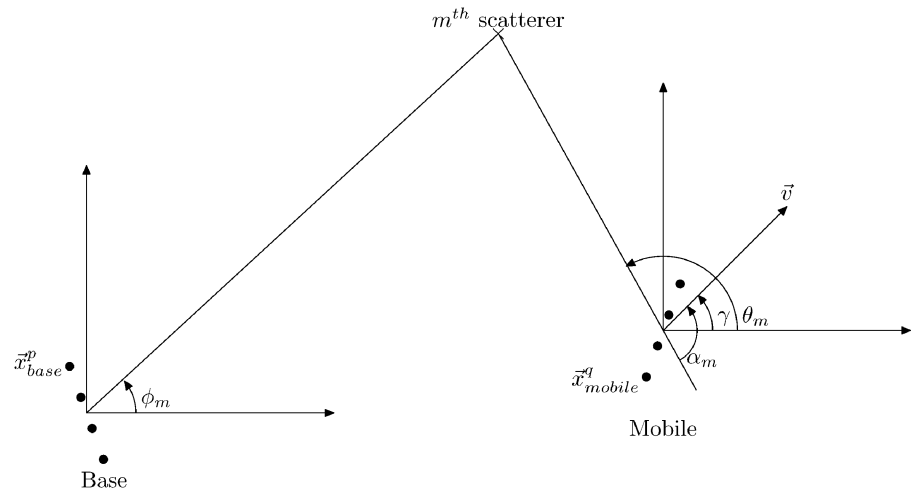


Fig. 1. Scattering model geometry.

$(-\pi, \pi)$ and independent of all other random quantities, we have

$$E\{h_{p,q}(t)h^*_{r,s}(t+\Delta t)\} = E\left\{\sum_{m=0}^{K-1} A_m^2 \exp[j2\pi f_c(-\tau_m(t)+\tau_m(t+\Delta t))] \times \exp\left[+j\vec{k}^m_{\text{base}}\cdot(\vec{x}^p_{\text{base}}-\vec{x}^r_{\text{base}})\right] \times \exp\left[+j\vec{k}^m_{\text{mobile}}\cdot(\vec{x}^q_{\text{mobile}}-\vec{x}^s_{\text{mobile}})\right]\right\}. \quad (23)$$

In order to specify the path delay associated with the $m$th scatterer, $\tau_m(t)$, some assumptions about the motion of the mobile must be made. In what follows, we assume a linear motion model. Specifically, the spatial location of the mobile as a function of time is given by

$$\vec{x}_{\text{mobile}}(t) = \vec{x}^0_{\text{mobile}} + \vec{v}t \quad (24)$$

with $\vec{x}^0_{\text{mobile}}$ denoting the initial location of the mobile and $\vec{v} = |\vec{v}|\cos(\gamma)$ denoting the velocity vector. The quantity $|\vec{v}|$ is the magnitude of velocity vector, and $\gamma$ is the angle the vector makes with the $x$-axis of the coordinate system. Using this model, the expression for the path delay is

$$\tau_m(t) = \frac{|\vec{x}_{\text{base}}-\vec{x}_m| + |\vec{x}_m - \vec{x}_{\text{mobile}}|}{c} = \frac{|\vec{x}_{\text{base}}-\vec{x}_m| + |\vec{x}_m - (\vec{x}^0_{\text{mobile}}+\vec{v}t)|}{c}. \quad (25)$$

In this expression, $c$ denotes the speed of light, and $|\vec{x}|$ denotes the norm of the vector $\vec{x}$. If $|\vec{x}^0_{\text{mobile}} - \vec{x}_m| \gg |\vec{v}t|$, the path delay can be approximated by

$$\tau_m(t) \approx \tau^0_m + \frac{|\vec{v}|t}{c}\cos\alpha_m \quad (26)$$

where $\tau^0_m$ corresponds to the static (time-invariant) portion of the path delay and $\alpha_m$ is the angle between the mobile velocity vector $\vec{v}$ and the line joining the initial mobile location and the location of the $m$th scatterer. In other words, the approximation to the path delay is appropriate if the distance traveled by the mobile at time $t$ is much less than the distance between the initial mobile location and the location of the $m$th scatterer.

Returning to the evaluation of the space-time correlation function (23) and employing the linear motion model for the mobile and the approximation developed for the path delay, we have

$$E\{h_{p,q}(t)h^*_{r,s}(t+\Delta t)\} = \exp(-j2\pi f_c\Delta t)E\left\{\sum_{m=0}^{K-1} A_m^2 \times \exp\left[j2\pi f_c\left(\frac{|\vec{v}|\Delta t}{c}\cos\alpha_m\right)\right] \times \exp\left[+j\vec{k}^m_{\text{base}}\cdot(\vec{x}^p_{\text{base}}-\vec{x}^r_{\text{base}})\right] \times \exp\left[+j\vec{k}^m_{\text{mobile}}\cdot(\vec{x}^q_{\text{mobile}}-\vec{x}^s_{\text{mobile}})\right]\right\}. \quad (27)$$

Define

$$\vec{x}^p_{\text{base}} - \vec{x}^r_{\text{base}} = d^{pr}_{\text{base}}(\cos\xi^{pr}_{\text{base}}, \sin\xi^{pr}_{\text{base}}, 0) \quad (28)$$

and

$$\vec{x}^q_{\text{mobile}} - \vec{x}^s_{\text{mobile}} = d^{qs}_{\text{mobile}}(\cos\xi^{qs}_{\text{mobile}}, \sin\xi^{qs}_{\text{mobile}}, 0). \quad (29)$$

The term $d^{pr}_{\text{base}}$ corresponds to the distance between the $p$th and $r$th array elements at the base, and $\xi^{pr}_{\text{base}}$ corresponds to the angle between the line joining the array elements and the $x$-axis. Similarly, $d^{qs}_{\text{mobile}}$ corresponds to the distance between the $q$th and $s$th array elements at the mobile, and $\xi^{qs}_{\text{mobile}}$ corresponds to the angle between the line joining the array elements and the $x$-axis.

Utilizing (20) and (21) and $\cos\alpha_m = -\cos(\gamma - \theta_m)$, (27) becomes

$$E\{h_{p,q}(t)h^*_{r,s}(t+\Delta t)\} = \exp(-j2\pi f_c\Delta t)E\left\{\sum_{m=0}^{K-1} A_m^2\right.$$

$$\times \exp[-j2\pi f_d \Delta t \cos(\theta_m - \gamma)]$$
$$\times \exp\left[+j\frac{2\pi}{\lambda} d^{pr}_{\text{base}} \cos(\phi_m - \xi^{pr}_{\text{base}})\right]$$
$$\times \exp\left[+j\frac{2\pi}{\lambda} d^{qs}_{\text{mobile}} \cos(\theta_m - \xi^{qs}_{\text{mobile}})\right]\Bigg\} \quad (30)$$

where $f_d = f_c(|\vec{v}|)/(c)$ corresponds to the maximum Doppler shift associated with the mobile. Given the array geometry at the mobile and the base station; the velocity vector associated with the mobile; and the joint probability density for $A_m$, $\phi_m$, and $\theta_m$, (30) can be used to compute the desired space-time correlation.

A special case of the previous result is of interest. Consider the case for which most of the scatterers are in the vicinity of the mobile. From the perspective of the base station, the angular spread of the multipath is small. Define $d = |\vec{x}^0_{\text{mobile}} - \vec{x}_{\text{base}}|$ and $R_m = |\vec{x}^0_{\text{mobile}} - \vec{x}_m|$. $d$ is the distance between the mobile and the base, and $R_m$ corresponds to the scattering radius associated with the $m$th scatterer. If $d \gg R_m$, then the angle $\phi_m$ can be approximated by

$$\phi_m \approx \frac{R_m}{d} \sin\theta_m \quad (31)$$

and

$$\cos\phi_m \approx 1$$
$$\sin\phi_m \approx \frac{R_m}{d} \sin\theta_m. \quad (32)$$

Evaluating (30) for the special case of *small angular spread* yields

$$E\{h_{p,q}(t)h^*_{r,s}(t+\Delta t)\}$$
$$= \exp(-j2\pi f_c \Delta t) \exp\left[j2\pi\left(\frac{d^{pr}_{\text{base}}}{\lambda}\cos\xi^{pr}_{\text{base}}\right)\right]$$
$$\times E\left\{\sum_{m=0}^{M-1} A_m^2 \exp\left[j2\pi\left(\frac{d^{qs}_{\text{mobile}}}{\lambda}\cos\xi^{qs}_{\text{mobile}}\right.\right.\right.$$
$$\left.\left. - f_d\Delta t\cos\gamma\right)\cos\theta_m\right]$$
$$\times \exp\left[j2\pi\left(\frac{d^{pr}_{\text{base}}}{\lambda}\frac{R_m}{d}\sin\xi^{pr}_{\text{base}}\right)\sin\theta_m\right]$$
$$\left.\times \exp\left[j2\pi\left(\frac{d^{qs}_{\text{mobile}}}{\lambda}\sin\xi^{qs}_{\text{mobile}} - f_d\Delta t\sin\gamma\right)\sin\theta_m\right]\right\} \quad (33)$$

In this result, the scattering geometry is specified by the joint probability distribution of the scattering radius about the mobile $R_m$ and the angle $\theta_m$ associated with the $m$th scatterer. The equation is applicable to arbitrary scattering geometry subject to the small angular spread approximation $d \gg \max\{R_m\}_{m=1}^M$.

Equation (33) describes the correlation between the transmission path from the $p$th transmit antenna to the $q$th receive antenna and the transmission path from the $r$th transmit antenna to the $s$th receive antenna with time separation $\Delta t$. In order to apply this result, the mobile velocity vector and initial distance from the base must be specified as well as the array geometry at the base and the mobile. Additionally, the joint probability distribution of the scatterer radius $R_m$ and angle $\theta_m$ with respect to the mobile must be given. In most cases of practical interest, (33) must be numerically integrated to yield a result. However, for the case of the circular ring scattering model attributed to Jakes [7], a closed-form expression for the complex path correlation can be obtained. This result is useful for validating the proposed space-time covariance model since it can be compared with previously published results. In the following section, we present numerical results for a 2-D Gaussian scattering model which is based upon measurements [19]–[22]. These results demonstrate the flexibility of the proposed space-time covariance model and provide a performance assessment of several space-time codes based upon a realistic scattering model.

For the Jakes model, the radius of each scatterer is fixed, i.e., $R_m = R$, and the angle of arrival $\theta_m$ is independent for each scatterer and uniformly distributed on $(-\pi, \pi)$. It is further assumed that the scatterer amplitude is fixed, i.e., $A_m = A$. With these assumptions, evaluating the expectation in (33) yields

$$E\{h_{p,q}(t)h^*_{r,s}(t+\Delta t)\}$$
$$= MA^2 \exp(-j2\pi f_c\Delta t)\exp\left[j2\pi\left(\frac{d^{pr}_{\text{base}}}{\lambda}\cos\xi^{pr}_{\text{base}}\right)\right]$$
$$\times J_0\left(2\pi\left[\left(\frac{d^{pr}_{\text{base}}}{\lambda}\frac{R}{d}\sin\xi^{pr}_{\text{base}}\right.\right.\right.$$
$$\left. + \frac{d^{qs}_{\text{mobile}}}{\lambda}\sin\xi^{qs}_{\text{mobile}} - f_d\Delta t\sin\gamma\right)^2$$
$$\left.\left. + \left(\frac{d^{qs}_{\text{mobile}}}{\lambda}\cos\xi^{qs}_{\text{mobile}} - f_d\Delta t\cos\gamma\right)^2\right]^{1/2}\right) \quad (34)$$

where $J_0(\cdot)$ denotes the zeroth-order Bessel function. This result is in agreement with that derived earlier in [11] for the special case of isotropic scattering and in [12].

To gain insight into the characteristics of the complex path correlation due to spatial and temporal effects for the Jakes model, consider the following special cases:

Case 1) $d^{pr}_{\text{base}} = 0 = d^{qs}_{\text{mobile}}$. This case corresponds to single transmit and receive antennas and considers only temporal correlation. The magnitude of the complex path correlation for this case is proportional to $|J_0(2\pi f_d\Delta t)|$. Uncorrelated space-time symbols result for normalized Doppler frequency $f_d\Delta t = 0.383$.

Case 2) $d^{qs}_{\text{mobile}} = 0, \sin\xi^{pr}_{\text{base}} = \pi/2$, and $\Delta t = 0$. This case corresponds to a single receive antenna and considers spatial correlation due to the spacing of the transmit antennas. The mobile is located broadside to the transmit antenna pair, and temporal effects are not considered. For this case, the magnitude of the complex path correlation is proportional to

$|J_0\left(2\pi d_{\text{base}}^{pr} R/(\lambda\, d)\right)|$. Note that the transmit antenna spacing required to achieve uncorrelated paths depends on the ratio of the scattering radius to the distance between the transmitter and receiver $R/d$. For the (unrealistic) case of $R/d = 1$, uncorrelated paths result for $d_{\text{base}}^{pr} = 0.383\lambda$. If $R/d = 0.01$, then a transmit antenna spacing of 38.3 $\lambda$ is required to achieve uncorrelated paths.

Case 3) $d_{\text{base}}^{pr} = 0$ and $\Delta t = 0$. This case corresponds to a single transmit antenna and considers spatial correlation due to the spacing of the receive antennas. Temporal effects are not considered. For this case, the magnitude of the complex path correlation is proportional to $|J_0\left(2\pi d_{\text{mobile}}^{qs}/\lambda\right)|$. The receive antenna spacing required to achieve uncorrelated paths is $d_{\text{mobile}}^{qs} = 0.383\lambda$ and does not depend on the scattering radius.

These special cases are in agreement with previous results due to Jakes and Clarke [7], [8].

## IV. Numerical Results

In this section, we evaluate the union bound on the block error probability (17) using a 2-D Gaussian scattering model for several space-time codes employing two and four transmit antennas and up to three receive antennas. Linear array geometry was employed at the base and mobile for all results. Variations in both spatial and temporal correlation are considered, and the results are compared to the case of an uncorrelated (space and time) channel.

The motivation for the use of the 2-D Gaussian scattering model is due to a recent measurement campaign conducted by Pedersen *et al.* [19]–[21] in which the temporal and azimuth dispersion of multipath in urban wireless environments was characterized. The study found that the power azimuth spectrum was accurately modeled using a truncated Laplacian function, and the power delay spectrum was well-approximated by a negative exponential function. Recent work by Janaswamy [22] concluded that the measurements reported by Pedersen *et al.* were consistent with a 2-D Gaussian model for the scatterer locations surrounding the mobile receiver.

The standard deviation of the scattering radius for the 2-D Gaussian model was varied from $\sigma_R = 10, 50, 200$ m, and the distance between the mobile and base (array phase centers) was fixed at $d = 1000$ m. The parameter $\sigma_R$ specifies the radius about the mobile for which approximately 68% of the scatterers are contained. The smallest value for $\sigma_R$ yields the ratio $\sigma_R/d = 0.01$ and corresponds to angular spread due to multipath of approximately $1^\circ$ from the perspective of the base station. The mobile location was broadside to the base antenna array, and its velocity was chosen such that the maximum Doppler frequency was approximately $f_d = 78$ Hz corresponding to a carrier frequency of 850 MHz and a maximum speed of 100 km/hr. Variations in the space-time symbol period $T_s$ were considered to assess the effects due to temporal correlation. Specifically, values used for the normalized Doppler frequency were $f_d T_s = 0.0033, 0.01, 0.05, 0.1$. The smallest value corresponds to a slow fading channel with a symbol to fading ratio of approximately 300:1. In other words, space-time symbols separated by 300 symbol periods are approximately uncorrelated. The largest value corresponds to a channel with a symbol to fading ratio of 10:1 and is denoted as fast fading.

The space-time block codes investigated include the orthogonal code [1]–[3], the orthogonal code with sphere packing [14], the diagonal algebraic code [4], and the cyclic code [5]. These codes were chosen because they respresent a wide spectrum of available space-time codes and yield reasonable performance.

For the presentation that follows, results for spatial correlation are presented first followed by the results for temporal correlation.

### A. Spatial Correlation

This section presents results for the slow fading ($f_d T_s = 0.0033$) and uncorrelated wireless channels with variations in spatial correlation due to transmit antenna spacing, receive antenna spacing and scattering radius standard deviation $\sigma_R$ for the 2-D Gaussian scattering model. Results for two transmit antennas are presented first followed by results for four transmit antennas. All results for two transmit antennas were evaluated at $10^{-2}$ block error probability, and all results for four transmit antennas were evaluated at $10^{-4}$ block error probability.

*1) Two Transmit Antennas:* For two transmit antennas, the orthogonal code due to Alamouti [1] was used with a 16-quadrature-amplitude modulation (QAM) symbol constellation. For the diagonal algebraic code, we also chose 16-QAM symbols and the unitary rotation matrix was chosen to be

$$\frac{1}{\sqrt{2}}\begin{pmatrix} 1 & e^{j\pi/4} \\ 1 & -e^{j\pi/4} \end{pmatrix}. \tag{35}$$

For all space-time codes, the spectral efficiency was 4 bits/s/Hz.

Fig. 2 shows the block error probability (union bound) versus SNR and scattering radius standard deviation for two transmit antennas ($\lambda/2$ spacing) and one receive antenna. The normalized Doppler frequency for this case was $f_d T_s = 0.0033$, representing slow fading. To achieve a block error probability of $10^{-2}$ for the uncorrelated channel, approximately 26.4 dB SNR is required for the diagonal algebraic code. The orthogonal code and orthogonal code with sphere packing realize performance improvements of 1.4 and 1.7 dB, respectively, over the diagonal algebraic code for the uncorrelated channel. For a scattering radius standard deviation of $\sigma_R = 10$ m, approximately 37.8 dB SNR is required to achieve a block error probability of $10^{-2}$ for the diagonal algebraic code. The orthogonal code and orthogonal code with sphere packing yield improvements of 0.4 dB and 0.7 dB, respectively, for this case. Thus, the channel with scattering radius standard deviation of $\sigma_R = 10$ m requires an increase in SNR of 11.4 dB, relative to that required for the uncorrelated channel, to achieve a block error probability of $10^{-2}$ for the diagonal algebraic code. The required increase in signal-to-noise ratio for the orthogonal code and the orthogonal code with sphere packing is 12.3 dB and 12.4 dB, respectively. These results highlight the dependence of space-time coding performance on spatial correlation for the slow fading channel.

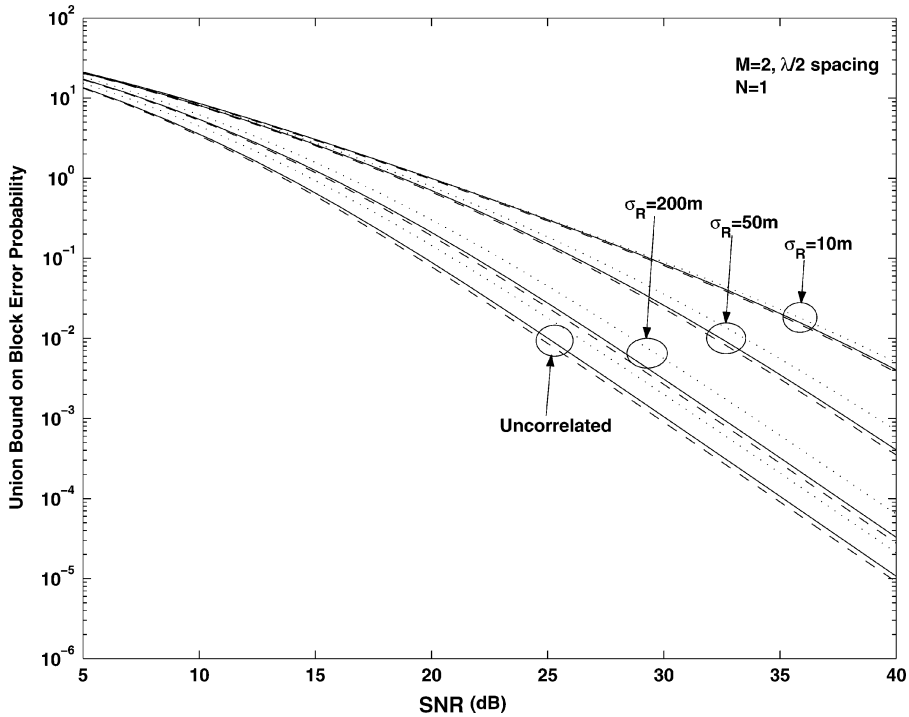


Fig. 2. Orthogonal code with 16-QAM symbols (solid curve), orthogonal code with sphere packing (dashed curve), diagonal algebraic code (dotted curve). Block error probability (union bound) versus SNR and scattering radius standard deviation, two transmit antennas ($\lambda/2$ spacing), one receive antenna, $f_d T_s = 0.0033$.

Fractional wavelength antenna spacing at the transmitter combined with small scattering radius yield transmission paths that are highly correlated and result in degraded performance relative to the uncorrelated channel. Increasing the spacing of the transmit antennas mitigates this effect to a certain extent as will be demonstrated next. Fig. 2 also illustrates that a diversity order of two is achieved for all space-time codes investigated for the uncorrelated channel. For example, the block error probability for the orthogonal space-time code and uncorrelated channel is reduced from $10^{-3}$ at a SNR of 30 dB to $10^{-5}$ at a SNR of 40 dB. Although not evident from the figure, it was verified that the asymptotic slope of the block error probability for the 2-D Gaussian scatterer model with $\sigma_R = 10,\ 50,\ 200$ m was the same as that for the uncorrelated channel, and thus these cases also yield a diversity order of two. For a scattering radius standard deviation of $\sigma_R = 10$ m, the asymptotic slope of the block error probability is realized for SNRs greater than 50 dB.

Fig. 3 shows the block error probability (union bound) versus SNR and transmit antenna spacing for a single receive antenna and normalized Doppler frequency of $f_d T_s = 0.0033$ and scattering radius standard deviation of $\sigma_R = 10$ m. From these results, it was determined that an antenna spacing of 30 $\lambda$ is required to achieve performance within 0.5 dB of the uncorrelated channel for $10^{-2}$ block error probability. For a carrier frequency of 850 MHz, the transmitted wavelength is $\lambda = 0.35$ m and 30 $\lambda = 10.5$ m. From Fig. 3, it is seen that increasing the spacing of the transmit antennas from $\lambda/2$ to 5 $\lambda$ decreases the SNR required to achieve a block error probability of $10^{-2}$ by 6.7 dB for the diagonal algebraic code, 7.4 dB and 7.5 dB, respectively, for the orthogonal code and orthogonal code with sphere packing for a scattering radius standard deviation of $\sigma_R = 10$ m.

Fig. 4 shows the results for two transmit antennas (5 $\lambda$ spacing) and two receive antennas ($\lambda/2$ spacing) and $f_d T_s = 0.0033$. A SNR of 17.3 dB is required to achieve a block error probability of $10^{-2}$ for the diagonal algebraic code and an uncorrelated channel. The orthogonal code and orthogonal code with sphere packing achieve gains of 0.6 dB and 1.1 dB, respectively, over the diagonal algebraic code for the uncorrelated channel. For the channel with scattering radius standard deviation $\sigma_R = 10$ m the required SNRs to achieve $10^{-2}$ block error probability are 20.7, 20.4, and 20.0 dB, respectively, for the diagonal algebraic code, orthogonal code, and orthogonal code with sphere packing. Comparing Figs. 3 and 4 it is seen that the addition of one receive antenna ($\lambda/2$ spacing) reduces the SNR required to achieve a block error probability of $10^{-2}$ by 9.1 dB for the diagonal algebraic code, 8.3 dB and 8.5 dB, respectively, for the orthogonal code and orthogonal code with sphere packing for the uncorrelated channel. Fig. 4 also illustrates that a diversity order of four is achieved for the uncorrelated channel, and for all space-time codes investigated. For example, the block error probability for the orthogonal space-time code is reduced from $10^{-7}$ at a SNR of 30 dB to $10^{-11}$ at a SNR of 40 dB. Although not evident from the figure, it was verified that the asymptotic slope of the block error probability for the 2-D Gaussian scatterer model with $\sigma_R = 10$ m was the same as that for the uncorrelated channel, and thus this case also yields a diversity order of four. For this case, the asymptotic slope of the block error probability is realized for SNRs greater than 40 dB.

*2) Four Transmit Antennas:* For the case of four transmit antennas, we investigated three space-time codes having a spectral efficiency of 2 bits/s/Hz. These codes are: the orthogonal code with sphere packing [13], [14], the cyclic code [5], and the

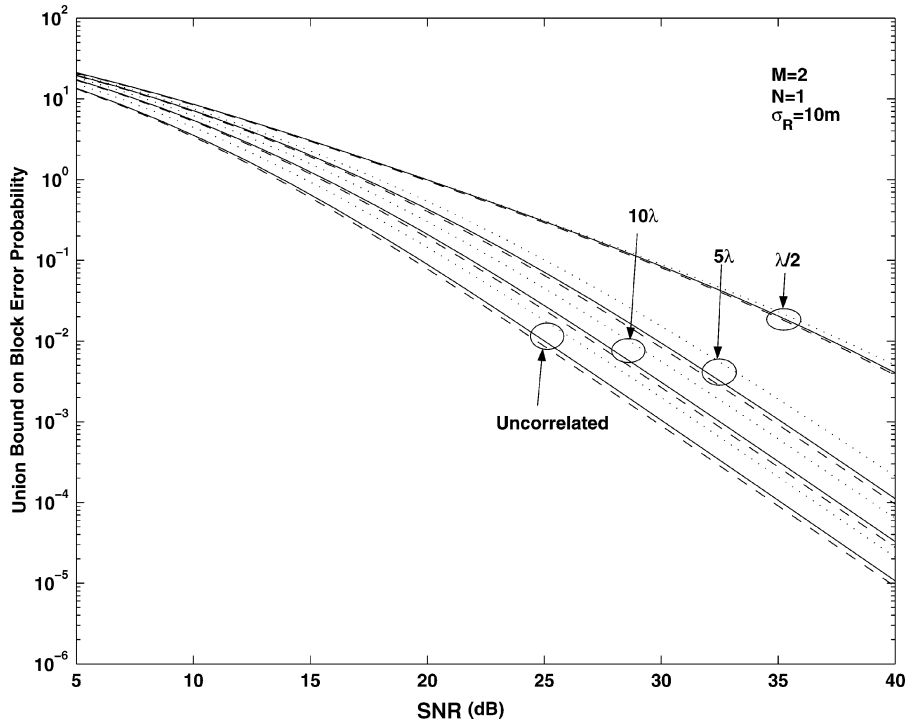


Fig. 3. Orthogonal code with 16-QAM symbols (solid curve), orthogonal code with sphere packing (dashed curve), diagonal algebraic code (dotted curve). Block error probability (union bound) versus SNR and transmit antenna separation, two transmit antennas, one receive antenna, $f_d T_s = 0.0033, \sigma_R = 10$ m.

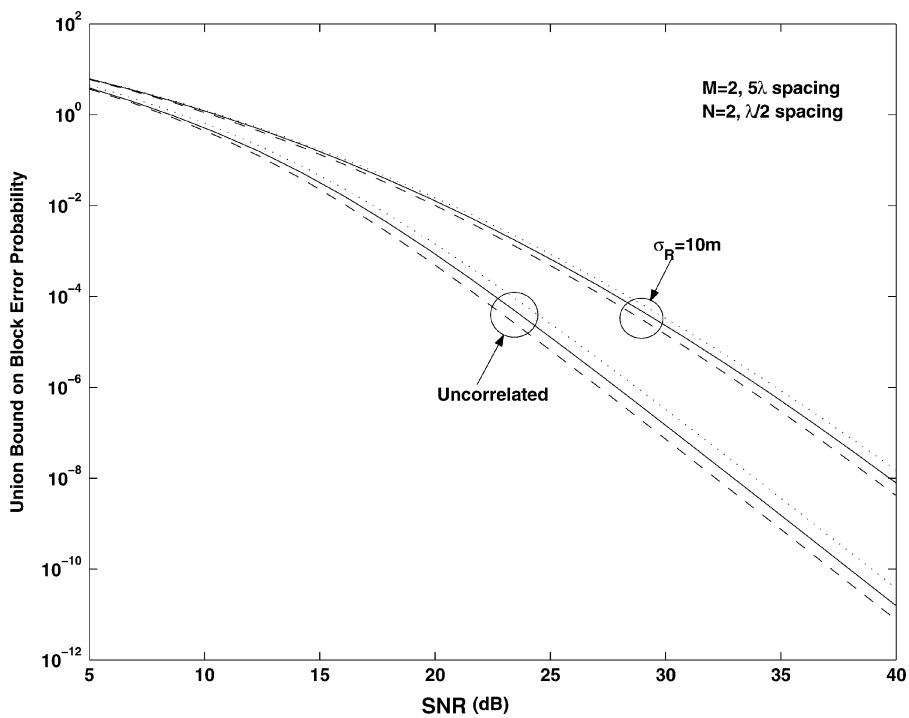


Fig. 4. Orthogonal code with 16-QAM symbols (solid curve), orthogonal code with sphere packing (dashed curve), diagonal algebraic code (dotted curve). Block error probability (union bound) versus SNR and scattering radius standard deviation, two transmit antennas ($5\lambda$ spacing), two receive antennas ($\lambda/2$ spacing), $f_d T_s = 0.0033$.

diagonal algebraic code with unitary rotation matrix

$$\frac{1}{2}\begin{pmatrix} 1 & e^{j\pi/8} & e^{j2\pi/8} & e^{j3\pi/8} \\ 1 & -e^{j\pi/8} & e^{j2\pi/8} & -e^{j3\pi/8} \\ 1 & je^{j\pi/8} & -e^{j2\pi/8} & -je^{j3\pi/8} \\ 1 & -je^{j\pi/8} & -e^{j2\pi/8} & je^{j3\pi/8} \end{pmatrix} \tag{36}$$

and QPSK signal constellation. Fig. 5 shows the block error probability (union bound) versus SNR and scattering radius standard deviation for four transmit antennas ($\lambda/2$ spacing) and one receive antenna. The normalized Doppler frequency for this case was $f_d T_s = 0.0033$, representing slow fading. To achieve

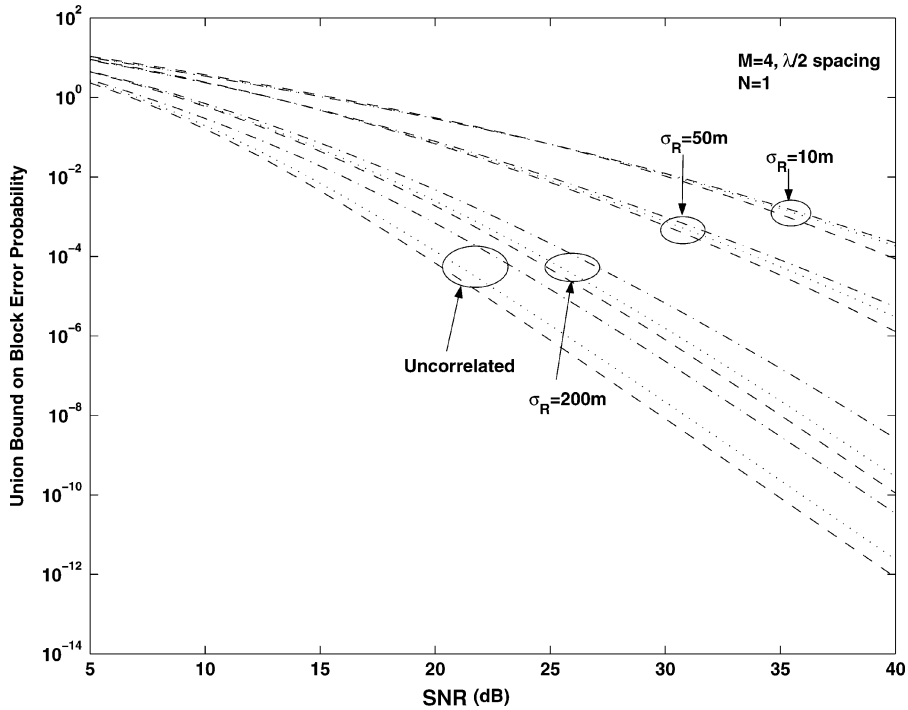


Fig. 5. Orthogonal code with sphere packing (dashed curve), diagonal algebraic code (dotted curve), cyclic code (dash-dotted curve). Block error probability (union bound) versus SNR and scattering radius standard deviation, four transmit antennas ($\lambda/2$ spacing), one receive antenna, $f_d T_s = 0.0033$.

a block error probablity of $10^{-4}$ for the uncorrelated channel, a SNR of approximately 22.6 dB is required for the cyclic code. The diagonal algebraic and the orthogonal code with sphere packing realize performance improvements of 2.2 dB and 3.0 dB, respectively, over the cyclic code for the uncorrelated channel. For a scattering radius standard deviation of $\sigma_R = 10$ m, approximately 41.7-dB SNR is required to achieve a block error probability of $10^{-4}$ for the cyclic code. The diagonal algebraic and the orthogonal code with sphere packing yield improvements of 0.4 dB and 2.0 dB, respectively, for this case. With reference to Fig. 5, note that 19.1 dB additional SNR is required to maintain a block error probability of $10^{-4}$ for a scattering radius standard deviation of $\sigma_R = 10$ m compared with the uncorrelated channel for the cyclic code. The diagonal algebraic code and orthogonal code with sphere packing require an additional SNR of 20.9 and 20.1 dB, respectively, for the same conditions. Fig. 5 also illustrates that a diversity order of four is achieved for the uncorrelated channel and for all space-time codes investigated. For example, the block error probability for the orthogonal space-time code with sphere packing is reduced from $10^{-8}$ at a SNR of 30 dB to $10^{-12}$ at a SNR of 40 dB. Although not evident from the figure, it was verified that the asymptotic slope of the block error probability for the 2-D Gaussian scatterer model with $\sigma_R = 10, 50, 200$ m was the same as that for the uncorrelated channel and thus these cases also yield a diversity order of four. For a scattering radius standard deviation of $\sigma_R = 10$ m, the asymptotic slope of the block error probability is realized for SNRs greater than 120 dB.

Fig. 6 shows the block error probability (union bound) versus SNR and transmit antenna spacing for scattering radius standard deviation $\sigma_R = 10$ m and normalized Doppler frequency $f_d T_s = 0.0033$. It was found that a transmit antenna spacing of 40 $\lambda$ (14.0 m) is required to achieve performance within 0.5 dB of that for the uncorrelated channel at a block error probability of $10^{-4}$. From Fig. 6, it is seen that increasing the spacing of the transmit antennas from $\lambda/2$ to 5 $\lambda$ decreases the SNR required to achieve a block error probability of $10^{-4}$ by 11.3 dB for the cyclic code and 11.9 and 10.9 dB, respectively, for the diagonal algebraic code and orthogonal code with sphere packing for a scattering radius standard deviation of $\sigma_R = 10$ m.

Figs. 7 and 8 show the results for two and three receive antennas ($\lambda/2$ spacing), respectively, and four transmit antennas (5 $\lambda$ spacing) for $f_d T_s = 0.0033$ and scattering radius standard deviation $\sigma_R = 10$ m and the uncorrelated channel. For the case of two receive antennas, the cyclic code achieves a block error probability of $10^{-4}$ at a SNR of 14.4 dB for the uncorrelated channel. A performance improvement of 1.8 and 2.0 dB, respectively, is observed for the diagonal algebraic code and orthogonal code with sphere packing for the uncorrelated channel. For the case of 3 receive antennas, the cyclic code achieves a block error probability of $10^{-4}$ at a SNR of 10.9 dB for the uncorrelated channel. A performance improvement of 1.3 and 1.4 dB, respectively, is observed for the diagonal algebraic code and orthogonal code with sphere packing for the uncorrelated channel. Comparing Figs. 6–8, it is seen that a system with two receive antennas requires 8.2 dB less SNR ratio to achieve a block error probability of $10^{-4}$ than a system with one receive antenna for the cyclic code and uncorrelated channel. It was found that a system with three receive antennas further reduces the required SNR by 3.5 dB compared with the case of two receive antennas for the same conditions. Also, results for four receive antennas (not shown) demonstrate a further reduction

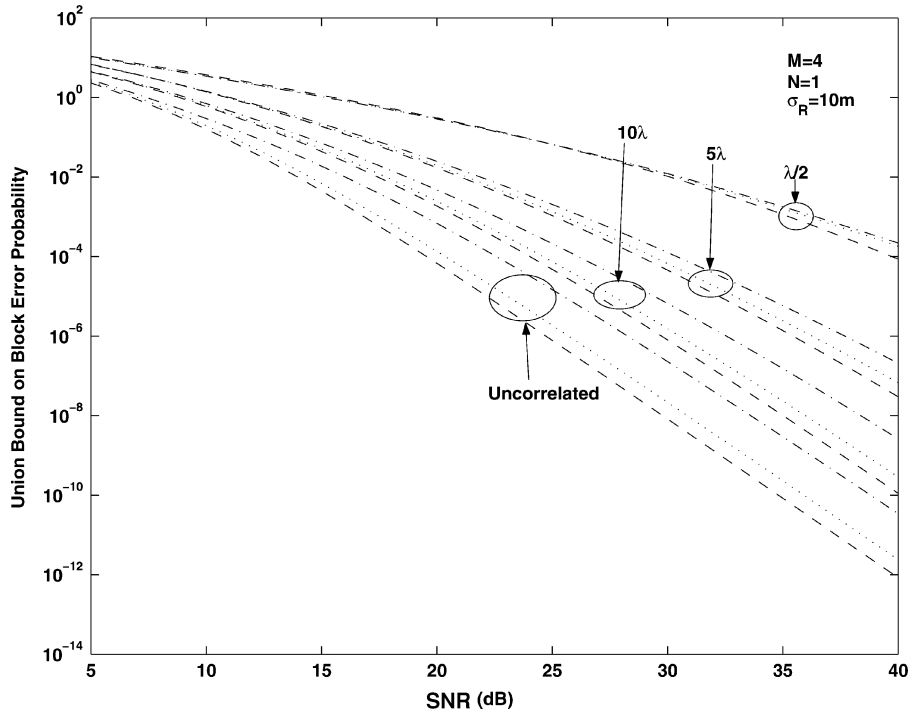


Fig. 6. Orthogonal code with sphere packing (dashed curve), diagonal algebraic code (dotted curve), cyclic code (dash-dotted curve). Block error probability (union bound) versus SNR and transmit antenna spacing, four transmit antennas ($\lambda/2$ spacing), one receive antenna, $f_d T_s = 0.0033, \sigma_R = 10$ m.

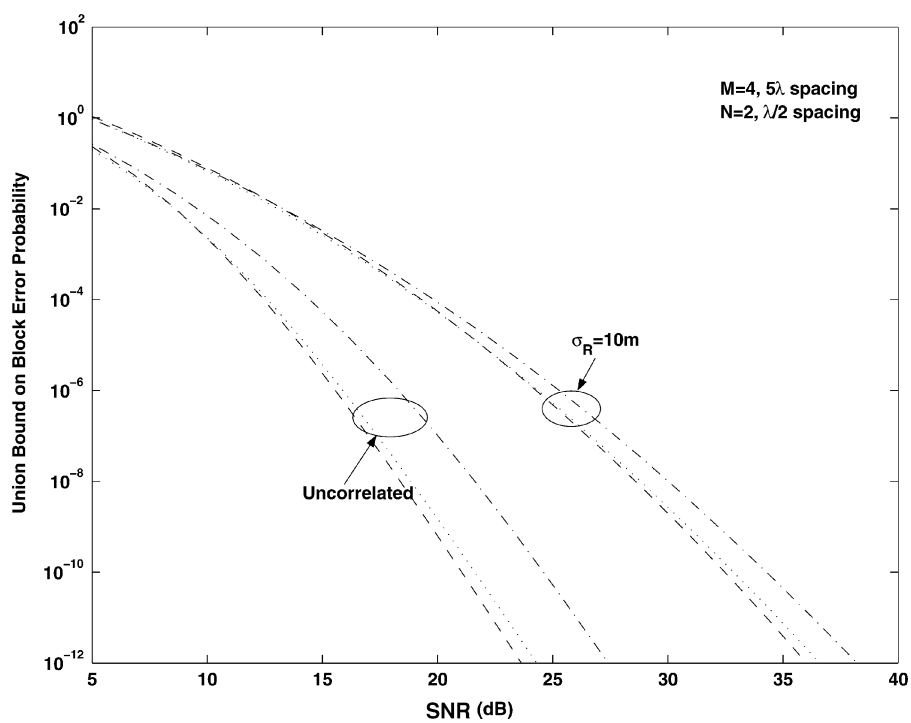


Fig. 7. Orthogonal code with sphere packing (dashed curve), diagonal algebraic code (dotted curve), cyclic code (dash-dotted curve). Block error probability (union bound) versus SNR and scattering radius standard deviation, four transmit antennas ($5\lambda$ spacing), two receive antennas ($\lambda/2$ spacing), $f_d T_s = 0.0033$.

of 2.1 dB compared with the case of three receive antennas. Although these comparisons were made for the cyclic code, comparable results were obtained for the diagonal algebraic code and orthogonal code with sphere packing. From these results, it appears that the benefit realized by adding multiple receive antennas diminishes with increasing numbers of antennas.

### B. Temporal Correlation

This section investigates the space-time block code error performance due to variations in temporal correlation. Four cases for the normalized Doppler frequency were considered, $f_d T_s = 0.0033, 0.01, 0.05, 0.1$. The smallest value corresponds to a slow fading wireless channel, and the largest value corresponds to the

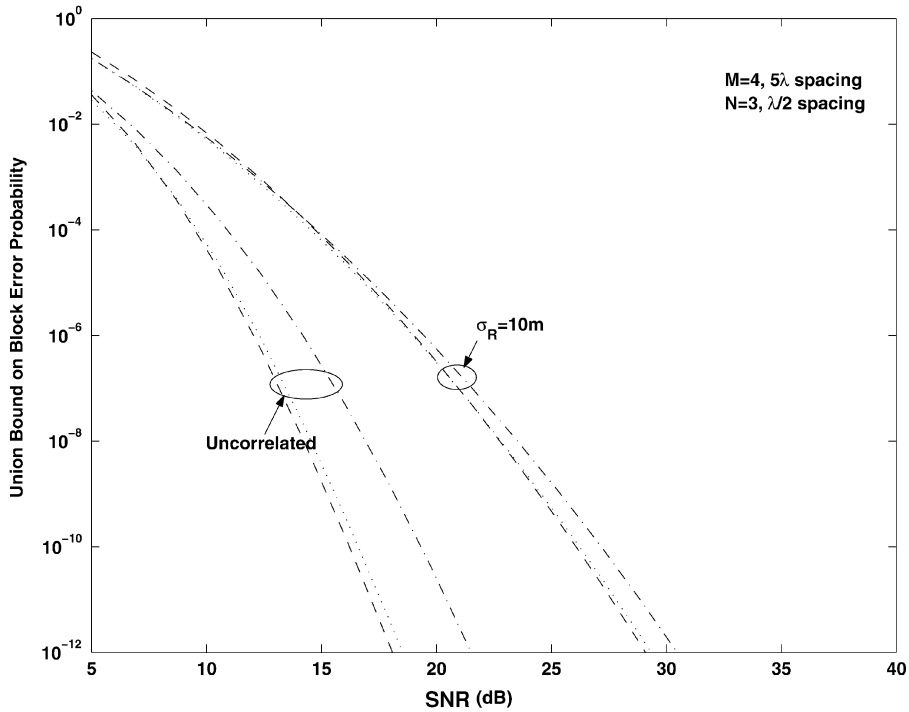


Fig. 8. Orthogonal code with sphere packing (dashed curve), diagonal algebraic code (dotted curve), cyclic code (dash-dotted curve). Block error probability (union bound) versus SNR and scattering radius standard deviation, four transmit antennas (5 $\lambda$ spacing), three receive antennas ($\lambda/2$ spacing), $f_d T_s = 0.0033$.

case of fast fading. The symbol to fading ratios for the slow fading and fast fading cases are 300:1 and 10:1, respectively. All results for two transmit antennas were evaluated at $10^{-2}$ block error probability, and all results for four transmit antennas were evaluated at $10^{-4}$ block error probability.

*1) Two Transmit Antennas:* Fig. 9 shows the block error probability (union bound) versus SNR and normalized Doppler frequency for two transmit antennas ($\lambda/2$ spacing), one receive antenna, and scattering radius standard deviation $\sigma_R = 10$ m. For the fast fading channel ($f_d T_s = 0.1$), the orthogonal code with sphere packing requires 31.9-dB SNR to achieve a block error probability of $10^{-2}$. The orthogonal code and diagonal algebraic code yield improvements of 1.0 and 2.1 dB, respectively, over the orthogonal code with sphere packing for the fast fading channel. This case corresponds to space-time symbols with low temporal correlation but high spatial correlation due to the fractional wavelength spacing at the transmitter and small scattering radius. For the slow fading channel ($f_d T_s = 0.0033$), the diagonal algebraic code requires 37.8 dB SNR to achieve a block error probability of $10^{-2}$. The orthogonal code and the orthogonal code with sphere packing yield improvements of 0.5 dB and 0.7 dB, respectively, over the diagonal algebraic code for this case. With reference to Fig. 9 and considering a block error probability of $10^{-2}$, the best performing space-time code for the fast fading channel ($f_d T_s = 0.1$) and the channel with normalized Doppler frequency of $f_d T_s = 0.05$ is the diagonal algebraic code. However, this code yields the worst performance among all codes investigated for the slow fading channel ($f_d T_s = 0.0033$), and the uncorrelated (space and time) channel. Evidently, the structure of the diagonal algebraic code permits greater coding gain than what is achievable with either the orthogonal code or the orthogonal code with sphere packing for wireless channels that exhibit low temporal correlation between space-time symbols but high spatial correlation between transmission paths. On the other hand, for wireless channels that are both spatially and temporally uncorrelated, the orthogonal code with sphere packing provides the greatest coding gain among the space-time codes investigated. Although not evident from the figure, it was verified that all space-time codes exhibit the same asymptotic slope of block error probability versus SNR for all values of normalized Doppler frequency investigated and thus have the same diversity order. For a normalized Doppler frequency of $f_d T_s = 0.0033$, the asymptotic slope of the block error probability is realized for SNRs greater than 50 dB.

Fig. 10 shows the block error probability (union bound) versus SNR and normalized Doppler frequency for two transmit antennas (5 $\lambda$ spacing), one receive antenna, scattering radius standard deviation $\sigma_R = 200$ m, and the uncorrelated channel. From Fig. 10, it is seen that increasing the spacing of the transmit antennas from $\lambda/2$ to 5 $\lambda$ combined with an increase in scattering radius standard deviation from $\sigma_R = 10$ m to $\sigma_R = 200$ m produces a channel with low spatial correlation and results in error performance indistinguishable from the uncorrelated (space and time) channel for all variations of normalized Doppler frequency that were investigated. This result implies that reducing the spatial correlation between transmission paths is itself sufficient to realize the full diversity and coding gains that are achievable for a particular wireless channel. With reference to Fig. 10, the diagonal algebraic code requires 26.4-dB SNR to achieve a block error probability of $10^{-2}$ and the orthogonal code and orthogonal

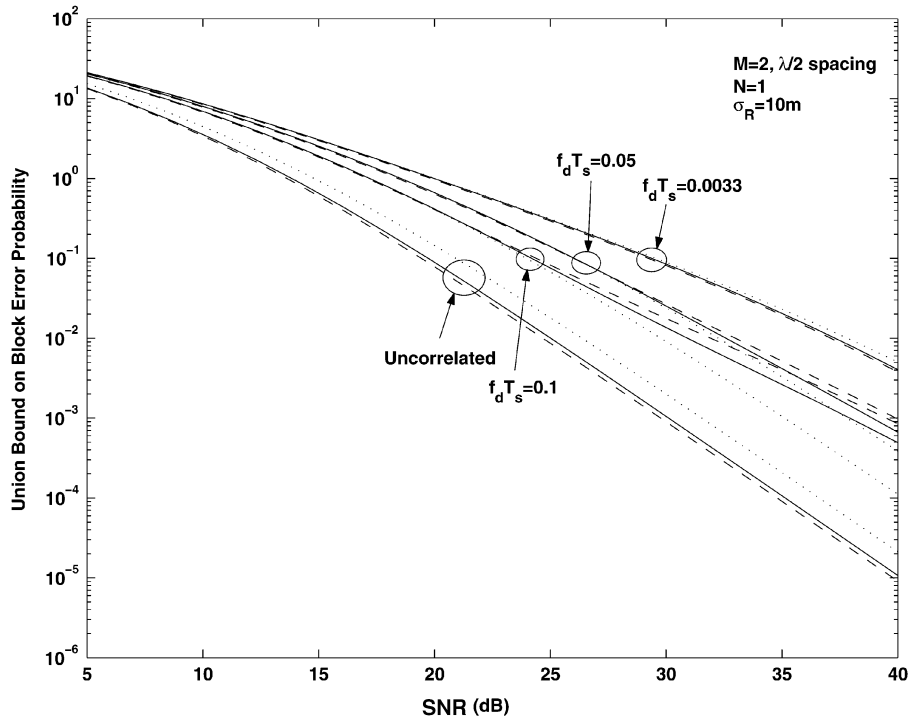


Fig. 9. Orthogonal code with 16-QAM symbols (solid curve), orthogonal code with sphere packing (dashed curve), diagonal algebraic code (dotted curve). Block error probability (union bound) versus SNR and normalized Doppler frequency, two transmit antennas ($\lambda/2$ spacing), one receive antenna, $\sigma_R = 10$ m.

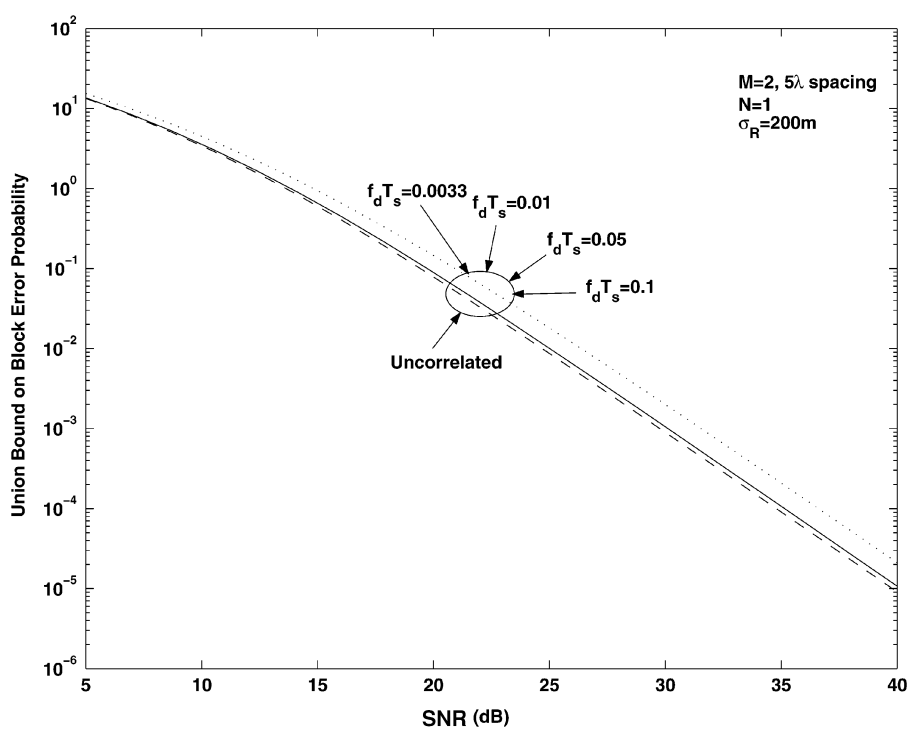


Fig. 10. Orthogonal code with 16-QAM symbols (solid curve), orthogonal code with sphere packing (dashed curve), diagonal algebraic code (dotted curve). Block error probability (union bound) versus SNR and normalized Doppler frequency, two transmit antennas ($5\lambda$ spacing), one receive antenna, $\sigma_R = 200$ m.

code with sphere packing provide improvements of 1.4 dB and 1.7 dB, respectively, over the diagonal algebraic code.

*2) Four Transmit Antennas:* Fig. 11 shows the block error probability (union bound) versus SNR and normalized Doppler frequency for four transmit antennas ($\lambda/2$ spacing), one receive antenna, scattering radius standard deviation $\sigma_R = 10$ m, and the uncorrelated channel. For the fast fading channel ($f_d T_s = 0.1$), the cyclic code requires 29.3-dB SNR to achieve a block error probability of $10^{-4}$. The orthogonal code with sphere packing and the diagonal algebraic code yield improvements of

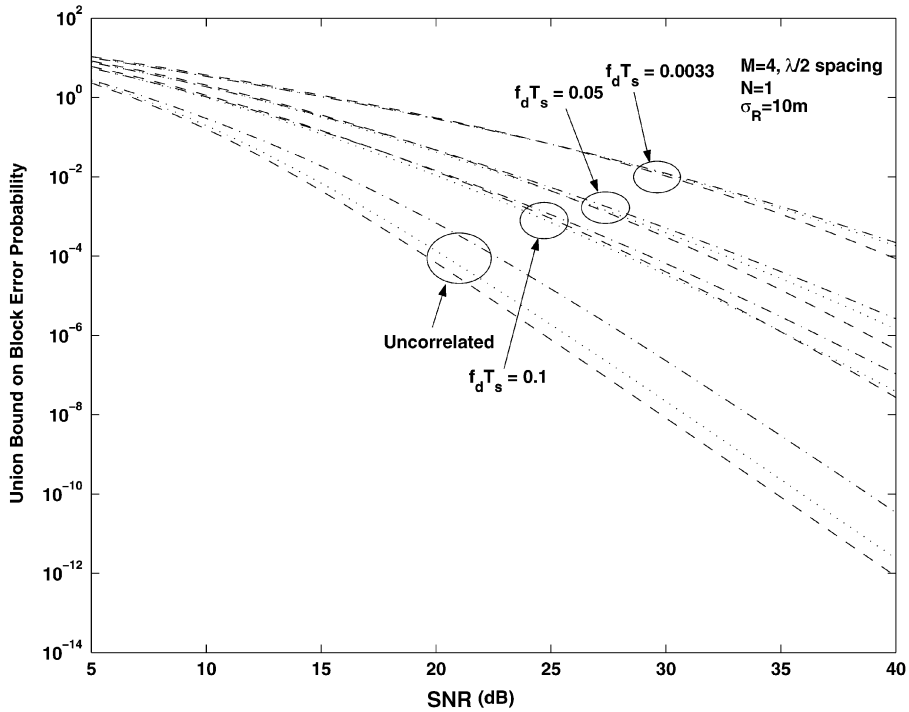


Fig. 11. Orthogonal code with sphere packing (dashed curve), diagonal algebraic code (dotted curve), cyclic code (dash-dotted curve). Block error probability (union bound) versus SNR and normalized Doppler frequency, four transmit antennas ($\lambda/2$ spacing), one receive antenna, $\sigma_R = 10$ m.

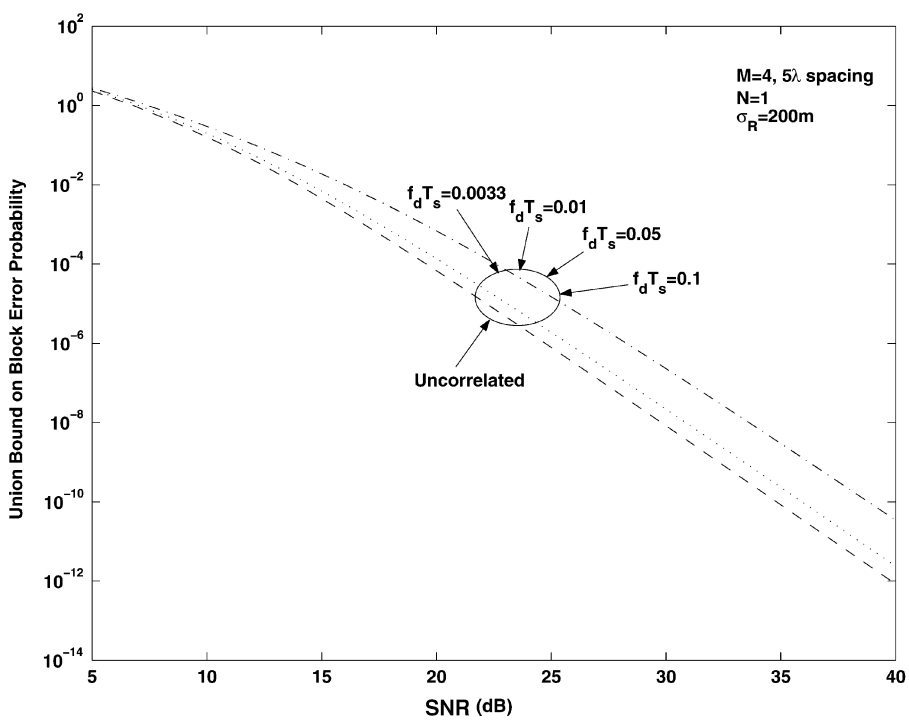


Fig. 12. Orthogonal code with sphere packing (dashed curve), diagonal algebraic code (dotted curve), cyclic code (dash-dotted curve). Block error probability (union bound) versus SNR and normalized Doppler frequency, four transmit antennas (5 $\lambda$ spacing), one receive antenna, $\sigma_R = 200$ m.

0.7 and 1.0 dB, respectively, over the cyclic code for the fast fading channel. This case corresponds to space-time symbols with low temporal correlation but high spatial correlation due to the fractional wavelength spacing at the transmitter and small scattering radius. For the slow fading channel ($f_d T_s = 0.0033$) the cyclic code requires 41.7 dB SNR to achieve a block error probability of $10^{-4}$. The diagonal algebraic code and the orthogonal code with sphere packing yield improvements of 0.4 and 2.0 dB, respectively, over the cyclic code for this case. Although not evident from the figure, it was verified that all

space-time codes exhibit the same asymptotic slope of block error probability versus SNR for all values of normalized Doppler frequency investigated and thus have the same diversity order. For a scattering radius standard deviation of $\sigma_R = 10$ m, the asymptotic slope of the block error probability is realized for SNRs greater than 120 dB.

Fig. 12 shows the block error probability (union bound) versus SNR and normalized Doppler frequency for four transmit antennas (5 $\lambda$ spacing), one receive antenna, scattering radius standard deviation $\sigma_R = 200$ m, and the uncorrelated channel. Comparing Figs. 11 and 12 it can be seen that increasing the transmit antenna separation and increasing the scattering radius standard deviation produces a channel with low spatial correlation and results in performance virtually indistinguishable from the uncorrelated (space and time) channel despite variations in the normalized Doppler frequency. With reference to Fig. 12 the cyclic code requires 22.7 dB SNR to achieve a block error probability of $10^{-4}$; the diagonal algebraic code and orthogonal code with sphere packing provide improvements of 2.1 and 2.9 dB, respectively, over the cyclic code.

## V. Conclusion

A general space-time covariance model has been proposed and used to investigate the robustness of several space-time codes for wireless channels that exhibit both spatial and temporal correlation. The best-case wireless channel for all space-time codes was uncorrelated in space and time.

For the slow fading wireless channel ($f_d T_s = 0.0033$), spatial correlation caused by fractional wavelength spacing at the transmitter or scatterers located in close proximity to the mobile resulted in significant performance degradation. For example, for the case of two transmit antennas there was roughly a 12-dB difference in SNR required (averaged over all space-time codes) to achieve $10^{-2}$ block error probability for the uncorrelated channel compared to the channel with scattering radius standard deviation $\sigma_R = 10$ m for $\lambda/2$ transmit antenna spacing. It was found that increasing the spacing of transmit antennas to 30 $\lambda$ (10.5 m) yielded performance within 0.5 dB of that for the uncorrelated channel for all space-time codes. For the case of four transmit antennas there was roughly a 20-dB difference in SNR required (averaged over all space-time codes) to achieve $10^{-4}$ block error probability for the uncorrelated channel compared to the channel with scattering radius standard deviation $\sigma_R = 10$ m for $\lambda/2$ transmit antenna spacing. For this case, it was found that increasing the spacing of transmit antennas to 40 $\lambda$ (14.0 m) yielded performance within 0.5 dB of that for the uncorrelated channel for all space-time codes. In some scenarios, it may impractical, due to physical constraints, for example, to achieve the transmit antenna spacing required for performance comparable to the uncorrelated channel. In such cases, some performance loss is inevitable and the results presented allow the performance degradation to be quantified.

Effects due to temporal correlation between adjacent space-time symbols resulting from mobile motion were also investigated. If the transmission paths are spatially correlated, a significant performance degradation is observed for slow fading ($f_d T_s = 0.0033$) compared to fast fading ($f_d T_s = 0.1$). For the case of two transmit antennas, there was roughly a 6.5-dB difference (averaged over all space-time codes) in the SNR required to achieve $10^{-2}$ block error probability for the fast fading channel compared to slow fading for scattering radius standard deviation $\sigma_R = 10$ m and $\lambda/2$ transmit antenna spacing. For the case of four transmit antennas, there was roughly a 12-dB difference in the SNR required (averaged over all space-time codes) to achieve $10^{-4}$ block error probability for the fast fading channel compared to the slow fading channel for scattering radius standard deviation $\sigma_R = 10$ m and $\lambda/2$ transmit antenna spacing. If the transmission paths are spatially uncorrelated, however, there is virtually no performance difference between the slow fading and fast fading channels. In fact, all variations in the normalized Doppler frequency that were investigated yield performance virtually indistinguishable to that observed for the uncorrelated (space and time) channel for this case.

The numerical results presented indicate that there exists a tradeoff between spatial correlation and temporal correlation effects in determining the performance of systems employing space-time block codes. The best-case wireless channel was found to be uncorrelated in both space and time. However, it was also determined that the effects of high spatial correlation may be compensated to a certain extent by low temporal correlation and vice versa to achieve performance comparable to the uncorrelated channel.

## References


[1] S. Alamouti, "A simple transmit diversity technique for wireless communications," *IEEE J. Sel. Areas Commun.*, vol. 16, no. 8, pp. 1451–1458, Oct. 1998.

[2] V. Tarokh, H. Jafarkhani, and A. R. Calderbank, "Space–time block coding for wireless communications: Performance results," *IEEE J. Sel. Areas Commun.*, vol. 17, no. 3, pp. 451–460, Mar. 1999.

[3] V. Tarkokh, H. Jafarkhani, and A. R. Calderbank, "Space-time block codes from orthogonal designs," *IEEE Trans. Inf. Theory*, vol. 45, no. 5, pp. 1456–1467, Jul. 1999.

[4] M. O. Damen, K. Abed-Meraim, and J.-C. Belfiore, "Diagonal algebraic space–time block codes," *IEEE Trans. Inf. Theory*, vol. 48, no. 3, pp. 628–636, Mar. 2002.

[5] B. M. Hochwald and W. Sweldens, "Differential unitary space–time modulation," *IEEE Trans. Commun.*, vol. 48, no. 12, pp. 2041–2052, Dec. 2000.

[6] J. Wang, M. K. Simon, M. P. Fitz, and K. Yao, "On the performance of space–time codes over correlated rayleigh fading channels," *IEEE Trans. Commun.* to be published.

[7] W. C. Jakes, *Microwave Mobile Commun.* Piscataway, NJ: IEEE Press, 1974.

[8] R. H. Clarke, "A statistical theory of mobile-radio reception," *Bell Syst. Tech. J.*, pp. 957–1000, Jul./Aug. 1968.

[9] T. A. Chen, M. P. Fitz, W.-Y. Kuo, M. D. Zoltowski, and J. H. Grimm, "A space–time model for frequency nonselective rayleigh fading channels with applications to space–time modems," *IEEE J. Sel. Areas Commun.*, vol. 18, no. 7, pp. 1175–1190, Jul. 2000.

[10] D. S. Shiu, G. J. Foschini, M. J. Gans, and J. M. Kahn, "Fading correlation and its effect on the capacity of multielement antenna systems," *IEEE Trans. Commun.*, vol. 48, no. 3, pp. 502–513, Mar. 2000.

[11] A. Abdi and M. Kaveh, "A space–time correlation model for multielement antenna systems in mobile fading channels," *IEEE J. Sel. Areas Commun.*, vol. 20, no. 3, pp. 550–560, Apr. 2002.

[12] Z. Safar and K.J.R. Liu, "Space–time correlation of MIMO flat rayleigh fading channels," in *Proc. EUSIPCO 2002*, Toulouse, France, Sep. 2002.

[13] W. Su and X.-G. Xia, "On space–time block codes from complex orthogonal designs," *Wireless Personal Commun.*, vol. 25, no. 1, pp. 1–26, 2003.
[14] W. Su, Z. Safar, and K. J. R. Liu, "Space–time signal design for time-correlated rayleigh fading channels," in *Proc. IEEE Int. Conf. Commun.*, vol. 5, May 2003, pp. 3175–3179.
[15] S. M. Kay, *Fundamentals of Statistical Signal Processing,* vol. II. Englewood Cliffs, NJ: Prentice-Hall, 1998.
[16] J. W. Craig, "A new, simple and exact result for calculating the probability of error for 2-D signal constellations," in *Proc. IEEE MILCOM Conf. Rec.*, Boston, MA, 1991.
[17] G. L. Turin, "The characterisitic function of hermitian quadratic forms in complex normal variables," *Biometrika*, pp. 199–201, 1960.
[18] S. Siwamogsatham, M. P. Fitz, and J. H. Grimm, "A new view of performance analysis of transmit diversity schemes in correlated rayleigh fading," *IEEE Trans. Inf. Theory*, vol. 48, no. 4, pp. 950–956, Apr. 2002.
[19] K. Pedersen, P. Mognesen, and B. Fleury, "A stochastic model of the temporal and azimuthal dispersion seen at the base station in outdoor propagation environments," *IEEE Trans. Veh. Technol.*, vol. 49, no. 2, pp. 437–447, Mar. 2000.
[20] K. Pedersen, P. Mognesen, and B. Fleury, "Power azimuth spectrum in outdoor environments," *Electron. Lett.*, vol. 33, no. 18, pp. 1583–1584, Aug. 1997.
[21] K. Pedersen, P. Mognesen, and B. Fleury, "Spatial channel characteristics in outdoor environments and their impact on the BS antenna system performance," in *Proc. IEEE Vehicular Technology Conf.*, 1998, pp. 719–723.
[22] R. Janaswamy, "Angle and time of arrival statistics for the gaussian scatter density model," *IEEE Trans. Wireless Commun.*, vol. 1, no. 3, pp. 448–497, Jul. 2002.

**Larry T. Younkins** (M'82) received the B.S. degree (*summa cum laude*) in electrical engineering from the University of Maryland, College Park, in 1982 and the M.E. degree from Cornell University, Ithaca, NY, in 1983. He received the Ph.D. degree in electrical engineering from the University of Maryland in 2004.

He was employed by AT&T Bell Laboratories from 1982–1986 and was involved in the design of telecommunication systems. From 1986 to the present, he has been employed with Applied Physics Laboratory, Johns Hopkins University, Laurel, MD. His research interests are many and include applications of signal processing to current problems in the areas of communications, navigation, and national defense.

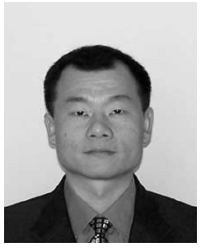

**Weifeng Su** (M'03) received the B.S. and Ph.D. degrees in mathematics from Nankai University, Tianjin, China, in 1994 and 1999, respectively. He also received the Ph.D. degree in electrical engineering from the University of Delaware, Newark, in 2002.

From June 2002 to March 2005, he was a Postdoctoral Research Associate with the Department of Electrical and Computer Engineering and the Institute for Systems Research (ISR), University of Maryland, College Park. Currently, he is an Assistant Professor with the Department of Electrical Engineering, State University of New York (SUNY) at Buffalo. His research interests span a broad range of areas from signal processing to wireless communications and networking, including space-time coding and modulation for MIMO wireless communications, cooperative communcations for wireless networks, and ultra-wideband (UWB) communcations.

Dr. Su received the Signal Processing and Communications Faculty Award from the University of Delaware in 2002 as an outstanding graduate student in the field of signal processing and communcations. He also received the Competitive University Fellowship Award from the University of Delaware in 2001. In 2005, he received the Invention of the Year Award from the University of Maryland. He serves as an Associate Editor for IEEE TRANSACTIONS ON VEHICULAR TECHNOLOGY.

**K. J. Ray Liu** (F'03) received the B.S. degree from the National Taiwan University, Taipei, Taiwan, R.O.C., in 1983, and the Ph.D. degree from the University of California Los Angeles, in 1990, both in electrical engineering.

He is Professor and Director of Communications and Signal Processing Laboratories of Electrical and Computer Engineering Department and Institute for Systems Research, University of Maryland, College Park. His research contributions encompass broad aspects of wireless communications and networking; information forensics and security; multimedia communications and signal processing; signal processing algorithms and architectures; and bioinformatics, in which he has published over 350 refereed papers.

Dr. Liu is the recipient of numerous honors and awards including IEEE Signal Processing Society 2004 Distinguished Lecturer, the 1994 National Science Foundation Young Investigator Award, the IEEE Signal Processing Society's 1993 Senior Award (Best Paper Award), IEEE 50th Vehicular Technology Conference Best Paper Award, Amsterdam, The Netherlands, 1999, and EURASIP 2004 Meritorious Service Award. He received the 2005 Poole and Kent Company Teaching Award from A. James Clark School of Engineering, University of Maryland, as well as the George Corcoran Award in 1994 for outstanding contributions to electrical engineering education and the Outstanding Systems Engineering Faculty Award in 1996 in recognition of outstanding contributions in interdisciplinary research from Institute for Systems Research. He is the Editor-in-Chief of *IEEE Signal Processing Magazine,* the prime proposer and architect of the new IEEE TRANSACTIONS ON INFORMAITON FORENSICS AND SECURITY, and was the founding Editor-in-Chief of *EURASIP Journal on Applied Signal Processing*. He is a Board of Governor at large of the IEEE Signal Processing Society.